Vaccine xxx (xxxx) xxx

Contents lists available at ScienceDirect

Vaccine

journal homepage: www.elsevier.com/locate/vaccine

Bacterial production of recombinant contraceptive vaccine antigen from CatSper displayed on a human papilloma virus-like particle

K.N. Nand [a,1], T.B. Jordan [a,1], X. Yuan [a], D.A. Basore [a,c], D. Zagorevski [a], C. Clarke [a], G. Werner [a], J.Y. Hwang [b], H. Wang [b], J-J. Chung [b,e], A. McKenna [d], M.D. Jarvis [d], G. Singh [d], C. Bystroff [a,*]

[a] Dept of Biological Sciences, Rensselaer Polytechnic Institute, Troy NY, United States
[b] Dept of Cellular and Molecular Physiology, Yale University School of Medicine, New Haven, CT, United States
[c] Department of Health and Natural Science, Mercy College, Dobbs Ferry, NY, United States
[d] Bioresearch Core, Rensselaer Polytechnic Institute, Troy, NY, United States
[e] Department of Gynecology and Obstetrics, Yale University School of Medicine, New Haven, CT, United States

ARTICLE INFO

Keywords:
Contraceptive vaccine
CatSper
Ca2+ ion channel

ABSTRACT

CatSper is a voltage dependent calcium ion channel present in the principal piece of sperm tail. It plays a crucial role in sperm hyperactivated motility and so in fertilization. Extracellular loops of mouse sperm CatSper were used to develop a vaccine to achieve protection from pregnancy. These loops were inserted at one of the three hypervariable regions of Human Papilloma Virus (HPV) capsid protein (L1). Recombinant vaccines were expressed in E.coli as inclusion body (IB), purified, refolded and assembled into virus-like particles (VLP) *in vitro*, and adsorbed on alum. Four vaccine candidates were tested in Balb/C mice. All the constructs proved immunogenic, one showed contraceptive efficacy. This recombinant contraceptive vaccine is a non-hormonal intervention and is expected to give long-acting protection from undesired pregnancies.

1. Introduction

The global unintended pregnancy rate between 2015 and 2019 was 48 %, and no region had unintended pregnancy rates below 25 %. [1] Unplanned pregnancies are caused either by contraceptive failure or non-use. Contraceptive failure is responsible for about half of unintended pregnancies. Long Acting Reversible Contraceptives (LARCs), require of the user no more than annual intervention, as opposed to barrier methods, spermicides, or daily oral contraceptives, which require perfect use daily or at every intercourse. LARCs have contraceptive failure rates 2-10 fold lower than other methods. [2–3] Contraceptive non-use is caused by a variety of factors, but 10 % of non-users in the US, and more than 20 % of non-users in 52 developing countries, cite concerns about side effects as the reason for nonuse. [4–5] Another frequently cited, though little studied, reason for nonuse is ideological objection to contraception. [5] Further, there are no reliably reversible, non-barrier methods of contraception available to male humans, despite interest from prospective users. [6] These data indicate demand for a novel contraceptive technology which is long-acting, reversible, and free of side effects. An anti-sperm contraceptive vaccine is likely to meet these criteria for both male and female humans. [7] Anti-sperm antibodies have no reported side effects, [8] have been shown to be contraceptive in humans, both male and female [9], and the contraceptive effect can last at least a year from the time of immunization. [10].

This paper describes proof of concept of such a vaccine, including design, expression, characterization of the particles, and vaccination studies in mice. CatSper (sperm-associated cation channel, GenBank: NP_647462, NP_001123502, NP_001239417, AAI08976) was selected as the antigenic target for the vaccine. Human Papillomavirus (HPV) type 11 major capsid protein L1 (L1, GenBank: ACL12350) was selected as the immunogenic carrier [18,19]. The results are chimeric proteins that assemble into virus-like particles.

The antigenic target protein, mouse CatSper (mCs), is a large hetero-oligomeric complex that is exclusively expressed on the principal piece of the sperm tail [11]. The opening of the voltage-dependent calcium ion channel activates hyperactivated motility, which is necessary for penetration of the extracellular matrix of the ovum. [12] Four genes, CatSper1-4, encode the pore-forming integral membrane subunits that are essential for male fertility. At least 4 additional CatSper-associated

* Corresponding author.
E-mail address: bystrc@rpi.edu (C. Bystroff).
[1] These authors contributed equally to the paper.

https://doi.org/10.1016/j.vaccine.2023.09.044
Received 15 November 2022; Received in revised form 19 September 2023; Accepted 20 September 2023

proteins (Genbank: NP_001355752, ACT09363, NP_001344826, ABO93459) are also essential for male fertility [11,13–14]. Consistent with these findings, the recent cryoelectron microscopy structure of the CatSper complex (called the *CatSpermasome;* PDBID:7eeb) includes CatSpers 1 through 4 along with CatSper-associated proteins β, γ, δ, and ε. The latter four proteins form a pavilion-like cover over the transmembrane pore-forming CatSper subunits (mouse CatSpers1-4, mCs1-4 in this manuscript) on the extracellular side [39]. Whole mCs1 and some of its extracellular loops have been shown to raise contraceptive antibodies [15], however, CatSper's large size and transmembrane components make the use of the whole protein impractical for injection as a vaccine. Instead, a subunit vaccine was conceived which would focus humoral immunity on the extracellular, antibody-accessible loops surrounding the site of calcium entry. Multiple sequence alignments and a homology-based model of CatSper [16] were used to predict the antigenic regions before the cryoEM structure was available. Four of the predicted antigenic regions were selected for a preliminary study, including two external sites on mCs1, one on mCs2, and one on mCsε.

The immunogenic carrier component of the vaccine, HPV11 L1 is a 56kD protein of the all-beta class that assembles into pentamers (*capsomeres*) which then assemble via a single disulfide link into a 360-mer icosahedral virus-like particle (VLP). L1 is expressed into the cytoplasm in the human host and is not natively glycosylated. HPV VLPs are thermodynamically stable [19] and have been used for more than a decade as a vaccine against HPV-associated cervical cancer [20]. Immunogenicity of the inserted CatSper epitopes is enhanced by their presentation on a VLP [18,49]. The immunogenicity, stability, manufacturability, and proven safety of L1 make it a good candidate as a carrier of peptidic haptens.

This paper describes the cloning, expression, purification, *in vitro* folding and assembly of VLPs, immunogenicity in mice, and the demonstrated contraceptive effect. Chimeric-L1 genes were synthesized using assembly PCR [21] and cloned into vectors using standard methods for expression in *E. coli*. The wild-type and chimeric L1 proteins were purified from inclusion bodies (IB), refolded by pulsed-flash dilution [45], and assembled *in vitro*. They were validated and characterized by SDS-PAGE, western blots, mass spectrometry, dynamic light scattering (DLS) and transmission electron microscopy (TEM). Mice were vaccinated with chimeric VLPs containing the four different loops from CatSper, showing the contraceptive effect in one case.

2. Materials and methods

2.1. Sequence and structure analysis

The protein sequences of twenty-three primate papillomavirus serotypes were aligned in Ugene [23] using MUSCLE [24]. Three-dimensional structures were analyzed, designed, and energy minimized using MOE (CCG, Montreal). The structure-based unfolding pathway of L1 was predicted using the GeoFold method [25], which identifies topologically possible pivot and hinge unfolding steps in a hierarchical manner, starting from the L1 capsomere structure (PDB: 2R5H). The folding pathway was taken to be the reverse of the predicted unfolding pathway.

Candidate antigenic loops from CatSper were selected based on the predicted or proven extracellular exposure. Three are located in the loops between transmembrane segments and one is located on one of the four CatSper-associated proteins that site on top of CatSper on the extracellular side (Fig. 1). Each candidate CatSper loop insertion was modeled using MOE's *loop design* function. Amino acid residues were added if necessary to avoid collisions. The conformations of the inserted loops were taken from the CatSper homology model [16] and were each treated as a rigid body during loop modeling. The CGP and GPC linkers were sampled in the disulfide linked state and were allowed to freely sample any structure, including *cis*-peptide conformations for the glycine-proline dipeptides. Five copies of the chimeric construct were assembled into a pentamer using MOE's *superpose* function and loops were energy minimized in place, leaving non-neighboring atoms fixed. Loop linkers were reconfigured if collisions were found upon generating the pentamer. Pentameric symmetry was enforced in the final model (Fig. 2).

2.2. Gene design and cloning

Two versions of HPV11 L1 [27] were made. In the first, called L1Δnls, the C-terminal twentyone residue nuclear localization sequence [28–29]was omitted. The second was the full length protein with restriction sites added around each of the three insertion sites in order to genetically "plug in" the peptide haptens, called "plug-in L1″ or piL1. Full gene sequences are provided in Supplemental Data. Overlapping oligonucleotides for assembly PCR synthesis were designed using DNAWorks [30]. Codon choice was optimized for *E. coli*. Oligonucleotides (IDT, Coralville, IA, USA) were assembled following the method of Stemmer [21] with minor changes; briefly, in a 25 ul reaction volume we used 100 fmol of each oligo and 1 pmol of the first forward and the last

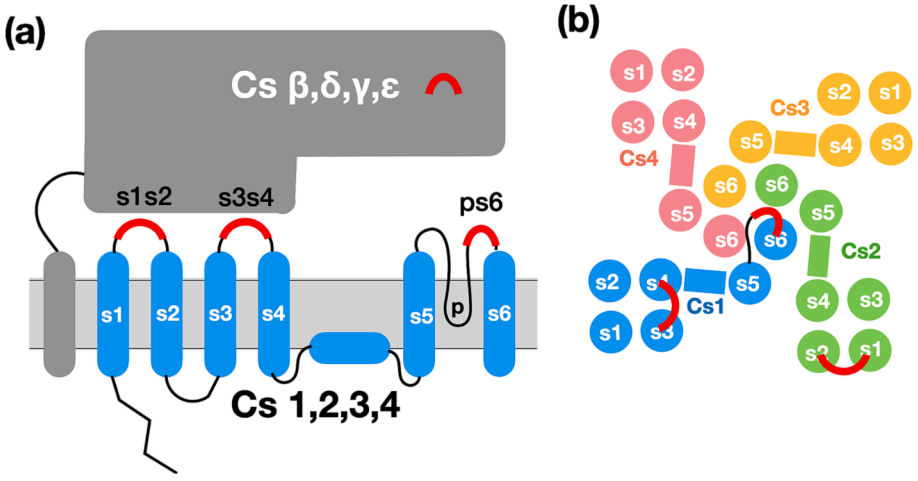

Fig. 1. Diagrammatic structure of sperm specific calcium channel CatSper, showing transmembrane segments s1 through s6 and large extracellular "pavilion" structure formed by CatSper-associated subunits β,γ,δ,ε. Red segments show where selected candidate epitope loops are located. (For interpretation of the references to colour in this figure legend, the reader is referred to the web version of this article.)

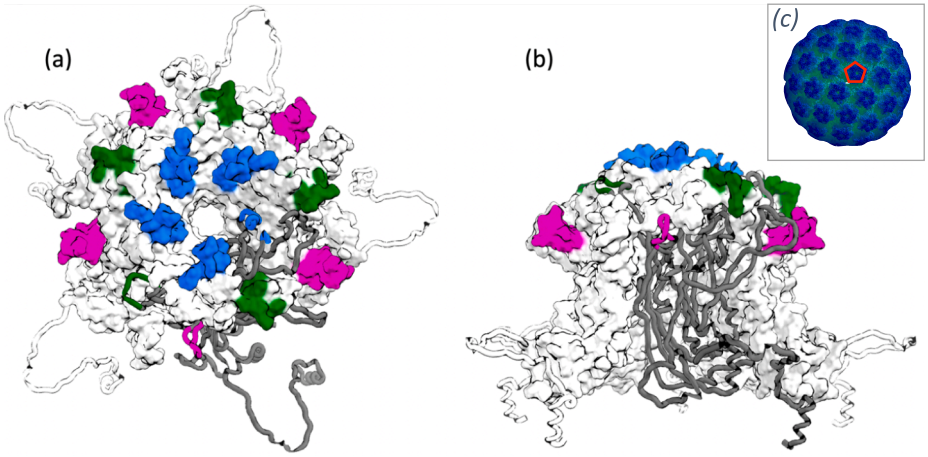

Fig. 2. HPV11 capsomere cryoEM structure 5KEP [22]. Three of the five hypervariable loops in are shown in pink (BC loop), blue (DE loop) and green (HI loop). One monomer is shown in grey ribbons, the other four as a molecular surface. (a) Top view. (b) Side view, capsid external face up. (c) 60 nm virus-like particle is composed of 72 capsomeres. (For interpretation of the references to colour in this figure legend, the reader is referred to the web version of this article.)

reverse oligos. Assembly generally produced about 1 μg pure amplicon after purification (E.Z.N.A. Cycle Pure Kit, Omega Biotech, Norcross, GA, USA).

The assembled genes were cut with restriction enzymes NdeI and EcoRI, ligated into the similarly digested pET28a + plasmid (Novagen Inc. Madison, WI, USA) with T4 DNA Ligase (New England Biolabs, Ipswich, MA, USA) and transformed into *E. coli* strain DH5α. Transformed cells were grown on luria broth (LB) agar plates with 50 μg/mL kanamycin overnight at 37 °C to yield colonies that were picked and grown overnight in 5 mL LB liquid cultures with 50 μg/mL kanamycin at 37 °C, shaking at 200 RPM. Plasmid was purified (E.Z.N.A Plasmid Mini Kit, Omega Biotek, Norcross, GA, USA) from these cultures, and the sequences were verified by Sanger sequencing (MCLAB, South San Francisco, CA, USA). The resulting plasmids are called pET28-L1, containing L1Δnls, and pET28-piL1, containing piL1 (See Supplementary Figure S2).

Table 1 lists the four constructs discussed here, called by their short names *p1*, *p2*, *c5*, and *s5*. Peptide hapten genetic inserts *p1* and *c5* were made by PCR amplifying the pET28-L1 plasmid using forward and reverse primers coding for the inserted loop and 20 bases of the flanking sequence. Constructs were verified by Sanger sequencing. The *p2* and *s5* inserts were made by assembling two oligonucleotides using PCR, followed by cutting with unique-cut restriction enzymes and ligating into the similarly digested piL1.

2.3. Expression and purification

Competent *E. coli* BL21(DE3) cells were transformed with the verified plasmids. Transformed BL21(DE3) cells were selected on LB agar plates with 50 μg/mL kanamycin. Individual colonies were used to inoculate 5 mL LB with 50 μg/mL kanamycin in 15 mL conical centrifuge tubes the grown at 37 °C, shaking at 200 rpm. Overnight cultures were used to inoculate 50 mL of LB in 500 mL Erlenmeyer flasks. The 50 mL cultures were grown to OD 0.6 at 37 °C, shaking at 200 rpm, then induced by adding isopropylthio-β-galactoside (IPTG) to a final concentration of 1 mM, then grown for another 4 h in the same conditions. Cells were harvested by centrifugation at 3600*g* and supernatants were discarded. Cell pellets were resuspended by gentle aspiration in 10 mL 50 mM NaCl, 50 mM tris pH 8 (lysis buffer) and lysed by 3 rounds of sonication. Each round of sonication consisted of cycles of 10 s on / 10 s off for a total of ten minutes. After each round of sonication, IB and cell debris were separated from soluble protein by centrifugation until the supernatant was clear, about 30 min at 13,000 g at 4 °C. The supernatants were decanted, and the post lysis pellets were washed thrice by resuspension in lysis buffer, centrifugation, and decanting.

The washed IB of constructs *c5* and *p1* were resuspended by stirring in 10 mL 8 M urea, 5 % beta mercaptoethanol (BME) for 2.5 h at room temperature to fully unfold the protein. The suspension was centrifuged for 20 min at 15,000 g to remove insoluble cell debris. IB of construct *s5* was resuspended by stirring in 2 mL 6 M guanidine hydrochloride (GuHCl), for 1 h, then centrifuged. The supernatant was diluted with 8 mL of 8 M urea. All constructs were > 0 % pure as shown on SDS-PAGE.

2.4. In vitro refolding and assembly

Folding was carried out by pulsed flash dilution [45]. The full 10 mL of each clear supernatant was diluted dropwise into 100 mL of vigorously stirred 50 mM tris, 50 mM NaCl, 100 mM Larginine, pH 9.0 (refolding solution), on ice. Care was taken during refolding to avoid the formation of foam by excessively vigorous stirring. The refolded L1 was

Table 1
Vaccine constructs tested. *p1* = mCs1_s3s4, *p2* = mCs2_s1s2, *c5* = mCsε_DGT, *s5* = mCs1_ps6. Underlined amino acids are mouse CatSper sequences. Others are linkers. Efficacy is defined as the number of females with zero-pup litters, versus total females. Mating experiment Rounds 1 and 2 used Balb/C mice. Round 3 used FVB/J mice. PBS (phosphate buffered saline) indicates the negative control experiments. § Failed negative control led to change of mouse strain. ‡ Round 3 mouse strain was FBV/J. nd = not done. *p = 0.0005. **p = 0.025.

ID	CatSper subunit	residues	HPV template	HPV insertion point	Inserted amino acid sequence	Contraceptive efficacy. zero-pup / total mice		
						1	2	3‡
p1	1	436–449	L1Δnls	BC	CGPNSLSYSFYNHSLFRGPC	7/8*	1/8	4/8**
p2	2	126–139	piL1	BC	CGPEIELMESTNTALWPGPC	1/8	nd	nd
c5	ε	331–348	L1Δnls	DE	CGPPDGTVYLRTEDEFTKLDESGPC	2/8	nd	nd
s5	1	542–554	piL1	HI	CGPYIDNRAQGAWYIIGPC	2/8	nd	nd
PBS	negative control					2/8	4/8§	0/8

centrifuged 20 min at 15,000*g* at 4 °C to remove aggregates, then dialyzed against 50 mM tris, 50 mM NaCl pH 8–10 to remove arginine, urea and BME. NaCl was added to a concentration of 500 mM to promote the formation of VLPs. All dialysis occurred on ice or at 4–10 °C, and transitions from one dialysis buffer to another were performed in gradual increments. The dialyzed L1 was spun for 20 min at 15,000*g*, 4° to remove aggregate.

2.5. SDS–PAGE and western blotting

Protein was resolved by gel electrophoresis using 10 % polyacrylamide and 0.1 % SDS (BIORAD, Hercules, CA, USA) [31]. Spectra Broad Range Multicolor Protein Ladder (ThermoFisher Scientific, Waltham, MA, USA) was used as a standard. Protein bands were stained by Coomassie Brilliant Blue R250 (Mallinkrodt Baker, Philipsburg, NJ, USA).

For Western blot analysis, proteins were resolved as above, then electro-transferred onto a nitrocellulose membrane [32] . The membrane was blocked with 3 % Bovine Serum Albumin (BSA), washed thrice in PBS, then rocked for one hour at room temperature with 1:3000 diluted CamVir1 (Invitrogen, ThermoFisher Scientific, Waltham, MA, USA), an anti-L1 mouse monoclonal antibody, then washed thrice in PBS and rocked for one hour, at room temperature with HRPlabelled goat anti-mouse IgG (Promega, Madison, WI, USA) diluted 1:6000. The membrane was washed 3 times with PBS buffer to remove unbound IgG. Immunoreactive bands were visualized with diaminobenzidine tetrahydrochloride (DAB) in the presence of hydrogen peroxide.

2.6. Transmission electron microscopy (TEM)

Refolded L1Δnls, *p1* and *c5* protein were each concentrated and buffer exchanged using centrifugal filters (Millipore, Burlington, MA, USA) to roughly 0.5 mg/mL in low salt (<50 mM NaCl). 0.5 µL of L1Δnls or *p1* was air dried onto a 300 mesh Carbon Type B grid (Ted Pella, Inc), for approximately 10 min. *s5* samples were not buffer exchanged to low salt, and were deposited onto grids in the dialysis buffer for 60 s, then excess solution was blotted away. All samples were stained with 2 % uranyl acetate solution for 60 s. Excess stain was blotted away gently. Images were collected using a JEOL 1200, or JEOL 2100 electron microscope, with an accelerating voltage of 200 kV. *p2* samples were prepared various ways but were of low quality on TEM.

2.7. Liquid chromatography tandem mass spectrometry (LCMSMS)

Samples were extracted from PAGE gels as described by Gundry [33], but without the final extraction in trifluoroacetic acid. LCMSMS experiments were performed on a Thermo LTQ Orbitrap XL (Bremen, Germany) mass spectrometer coupled with Agilent 1200 HPLC system (Agilent, Palo Alto, CA, USA). Samples were injected using an autosampler and the separation of peptides was performed on Thermo Accucore column 150x2.1 mm 2.6µ. Full scan mass spectra were collected on the orbitrap in m/z 400–1,000 range at resolution of 30,000 and with mass accuracy better than 3 ppm. Data dependent data acquisition was performed in the ion trap to obtain MS/MS spectra of two most intense peaks in the full scan. Only doubly- and triply-charged ions were subjected to collision induced dissociation (CID). Data base search was done using Trans-Proteomic Pipeline software [34]. The decoy data base was generated by reversing protein sequences. The false discovery rate (FDR) was set up to 1 %.

2.8. Dynamic light scattering (DLS)

1 mL samples of VLPs in dialysis buffer in polystyrene cuvettes were analyzed on an AntonPaar Litesizer 500 using Calliope software (AntonPaar, Graz, Austria) to determine the distribution of particle sizes in solution. Each sample was allowed to equilibrate in the beam for 2 min and data was collected cumulatively over 6 to 10 s samplings using side angle detection.

2.9. Immunization

Purified chimeric L1 proteins *p1*, *p2*, *c5*, and *s5* were transferred to PBS pH 6.8, incubated with 2 % alhydrogel (Brenntag) in 1:1 proportion on a nutator mixer at a 20° tilt angle (Marshall Scientific) at 4 °C overnight. Unabsorbed antigen was followed by checking the A280 of the supernatant. 6–8-week-old female Balb/C mice (Taconic Biosciences) were randomly divided into five different groups (n = 8). Each group of 8 mice received three primary immunizations at 15-day intervals, each one containing 5 µg alum-adsorbed vaccine, *p1*, *p2*, *c5*, or *s5*. One control group of 8 was injected with phosphate buffered saline (PBS). Body weight and other physical parameters of immunized and control group were monitored and recorded. Mice were housed in individually ventilated cages on a 12:12 light cycle. Environmental conditions were kept within ranges described in *Albus* [48]. All procedures performed were approved by the Institutional Animal Care and Use Committee at Rensselaer Polytechnic Institute.

2.10. Sera collection

Pre-immunization blood was collected and repeated at 15-day intervals using submandibular puncture. Sera was separated by incubating blood at room temperature followed by centrifugation and stored frozen till assays were carried out.

2.11. Mating experiment

Three rounds of mating experiments have been carried out so far. Groups of immunized female mice were co-housed with non-vaccinated healthy male mice 73 days post immunization. Two immunized females were allowed to mate with one normal male mouse in a cage. The mating experiment continued for three consecutive ovulatory cycles. Mating was monitored by checking the vaginal copulatory plug. Male and female mice were separated after three ovulatory cycles. Female mice were euthanized by CO_2 overdose and blood was collected via cardiac puncture, followed by cervical dislocation. During necropsy, fetal implantation sites (viable and non-viable fetuses) were counted in the uterine horns.

2.12. ELISA

Enzyme-linked immunosorbent assay (ELISA) was performed in 96 well microtiter plate (Thermo Fisher Scientific). Wells were coated with 100 ng/100ul/well of purified antigen overnight at 4 °C. Incubated wells were washed thrice with phosphate buffer saline with 0.05 % Tween 20 (PBST). 2 % BSA (bovine serum albumin) in PBS was incubated in each well at 37° for 1 hr to block non-specific binding. After washing thrice with PBST, wells were incubated at 37° for 1 hr with 100 mL of diluted serum. Post incubation wells were washed again and incubated with goat anti mouse IgG at 1:5000 dilution and incubated at 37° for 1 hr. OPD (orthophenylenediamine) in citrate phosphate buffer, pH 5.5 was used as substrate after washing the wells. The reaction was stopped with 5 N H_2SO_4 and absorbance was measured at 490 nm using a Absorbance 96 Plate Reader (Enzo Life Sciences).

Significance of OD measurements versus controls (mice injected with PBS) was calculated using the 1-tailed, unpaired T-test, which works best for small sample sizes [52]. The 1-tailed test is appropriate because the control ODs are very close to zero and negative ODs are not possible, thus the data is 1-tailed. The choice of using paired versus unpaired data was arbitrary since Day 1 ODs for injected mice (paired data) and Day 30 ODs for uninjected mice (unpaired) are statistically identical.

3. Results and discussion

3.1. Insertion sites and antigenic loops, selection and modeling

The success of a chimeric subunit vaccine strategy depends on the extent to which folding and assembly of the particle-forming protein are preserved, and the displayed loop is natively folded. Therefore the structural consequences of loop insertion were considered with regard to folding and assembly of the host L1 protein. L1 is a 55 kD, all beta, "jelly roll" fold which assembles into pentameric capsomeres via beta hairpin loop intercalation. A total of 72 capsomeres assemble into a spherical, 60 nm VLP, with T = 7d icosahedral symmetry [46,47]). Candidate locations for loop insertion were regions that are weakly conserved, especially where insertions and deletions occur (Fig. 3), and which were predicted to fold late and are relatively uninvolved in the assembly of the VLP. In the nucleation/propagation model for greek-key protein folding (Fig. 4), the EF loop is the folding initiation site, despite having one highly variable loop region (site 3 in Fig. 3). Following propagation of the antiparallel contacts to form a long hairpin structure, conserved loops CD and GH then bend cooperatively to form the right-handed, doublestrand cross-over that defines the greek key fold. At this point in folding, variable loops BC, DE, GH and HI are approximately lined up on one side of the protein (Fig. 4c) where they bend cooperatively in two places to complete the folding of the monomer. Most of the contacts to the variable loops are either with other variable loops or they are exposed to solvent. This means that sequences inserted into these locations are not engaged in folding until late in the pathway (miliseconds to seconds after folding initiation), and prior to that are free to adopt a conformation based on their own intrinsic, local sequence preferences [42]. CatSper loops were chosen so that they had a good number of local contacts to guide their folding; bent structures rather than extended ones. They were inserted genetically into L1Δnls or piL1 at BC, DE, and HI (Figs. 3 and 4).

Putative antigenic loops from CatSper were selected on the basis of published results in which mouse CatSper 1 extracellular loop s3s4 (mCs1_s3s4) and mouse CatSper1 extracellular loop ps6 (mCs1_ps6) (Fig. 1) were found to raise contraceptive immunity [26,15]. Mouse CatSper ε loop 331–346 (mCsε_DGT) was identified by antigenicity score. Antibodies raised to mCs1_s3s4 and mCsε_DGT labeled live sperm (Supplementary Fig. S1A); mCs1_ps6 was not tested. Twelve other CatSper loops have been considered, and ten have been cloned into L1 sites BE, DE or HI as listed in Table S1, but these have not yet been biophysically characterized or injected into mice.

3.2. Structurally native loop presentation

Native presentation of the antigenic loop is important during B-cell maturation in the germinal centers where undigested antigens are presented to hypermutated B-cell receptors for affinity selection [41]. If the antigenic loop is displayed in a non-native conformation, then the antibodies produced by those B-cells will not bind as tightly (or at all) to the true native state, in this case native CatSper.

It is possible to favor the native conformation of a polypeptide loop by placing it in the right context within a carrier protein. In this case, the CatSper loops were reverse turns (loop termini near each other) in the homology modeled CatSper structure [16], therefore they were inserted into regions of L1 where they would be forced to adopt a reverse turn structure. The reverse turn state was further stabilized using a disulfide bond at its base using the motif CGP-XGPC, where X denotes the inserted peptide. This motif has been shown to accept the insertion of arbitrary 12-residue peptides into thioredoxin without disrupting the protein tertiary structure [17]. We have found that the CGP-X-GPC improved expression of a chimeric L1 having a large insertion in the DE loop over that of a similar construct that had no disulfide linkage (unpublished data). We observed that the addition of the disulfide motif significantly increased expression levels. This was interpreted to mean folding was improved.

3.3. Physiological effect of antibodies against KLH-linked CatSper loops

In preliminary experiments, some of the CatSper antigens were each conjugated N-terminally to keyhole limpet hemocyanin (KLH) for generation of antibodies in rabbits. The resulting antibodies labeled fixed mouse sperm cells and also bound the corresponding CatSper subunits in a western blot. Some of the antibodies (see Supplementary Figure S1) also bound to live sperm cells in the principal piece of the tail where CatSper is known to be expressed. No nonspecific binding was observed in tests using CatSper knock-out mice. However, these antibodies did not significantly affect the motility of the sperm. This seems to contradict previously published results in which antibodies raised against the full length mCs1 reduced the pregnancy rate in mice by 80 % [15], implying a robust antibody effect on CatSper function. The recently solved "CatSpersome" cryoEM structure [39] partially explains the seeming contradiction. In short, not all of the epitopes are surface-exposed in that

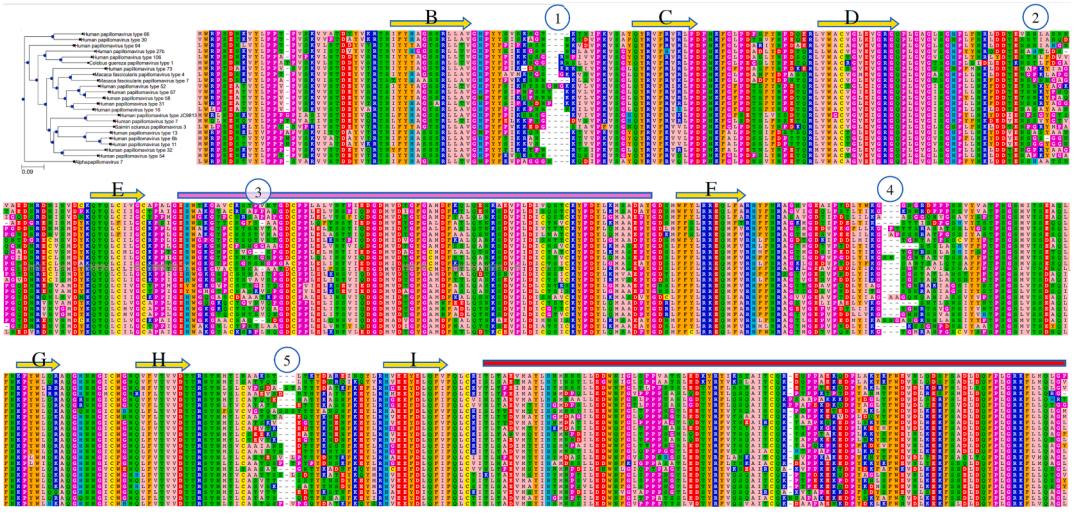

Fig. 3. Multiple sequence alignment for 23 primate papillomavirus L1 sequences. The core elements of secondary structure are labelled B through I, in accordance with canonical labelling of Jelly-roll proteins. The purple bar denotes the "irregular" domain, and the red bar denotes the invading arm. Circled numbers indicate loop regions with tolerance for indels. Such regions are good candidates for the insertion of foreign peptides in vaccine design. (For interpretation of the references to colour in this figure legend, the reader is referred to the web version of this article.)

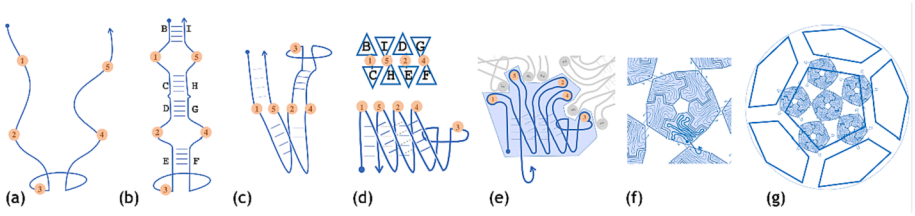

Fig. 4. A working hypothesis for the folding and assembly of HPV-L1 showing locations of 5 hypervariable loops; generated based on capsomere structure (PDB:2R5H) using GeoFold [25]. (a) Folding initiates at long EF loop, (b) a long hairpin forms by propagating antiparallel beta hydrogen-bonds through EF, DG, CH, BI strand pairs in that order, (c) short loops CD and HG hinge, (d) variable loops 1 and 5 hinge, variable loops 2 and 4 hinge forming a greek key structure having two antiparallel sheets with strand orders CHEF and BIDG, (e) variable loops intercalate to form a dimer, trimer and finally, capsomeres, (f) the five C-terminal "invading arms" link a central capsomere to five others via a disulfide linkage forming groups of 6 capsomeres, (g) 12 groups of 6 form a virus-like nanoparticle, via invading arm disulfide links.

structure. The structure suggests that antibody binding to multiple epitopes may be required to affect a change in CatSper function. A vaccine based on KLH-conjugated peptides was not further pursued because it would not be scalable to production level.

3.4. CatSper loop insertion into HPV L1 gene

Three insertion sites on HPV L1, the BC, DE and HI loops, were selected for experimental studies. CatSper1 (UniProt Q91ZR5) s3s4 loop 436-NSLSYSFYNHSLFR-449 replaced BC loop residues 52-KKVNKT-57 of L1 (UniProt ACL12350). CatSper ε (UniProt P0DP43) 331-DGTVYLRTEDEFTKLDES-348 was inserted in the DE loop between residues G133 and G134. And CatSper1 ps6 loop 542-YIDNRAQGAWYII-554 replaced L1 residues 343-ASVSYSATYT-352 in the HI loop. Each inserted loop was flanked by linker sequences as noted in Table 1. For full sequences, see Supplementary Data.

The L1Δnls gene was synthesized by assembly PCR [21] and cloned into pET28a +. Insertions were made by inverse PCR using oligonucleotides which coded for the inserted sequence, to form the chimeric constructs (see Supplementary Figure S2). Non-chimeric L1Δnls and each of the chimeric L1Δnls constructs lacked the highly-charged C-terminal 21-residue nuclear localization signal (NLS), as a precaution, since the presence of the NLS effects expression of VLPs in chloroplasts [44]. The L1Δnls constructs contained an N-terminal 6-his tag; it was not used for purification purposes because the protein isolated from IB was already pure enough.

"Plug-in" cL1 (piL1) was constructed to allow for the easy swapping of loops into L1. Unique restriction sites were placed before and after each of three sites (BC, DE, and HI). DNA fragments coding for the desired inserts were assembled from oligonucleotides [21], cut with the appropriate enzymes and ligated into similarly cut piL1 vector to create each cL1. VLPs made using piL1 do not appear to be different from cL1′s based on L1Δnls, indicating that the minor sequence changes are non-consequential.

3.5. Expression and purification

Protein was expressed in recombinant *E coli* grown in LB at 37 °C and induced with 1 mM.

IPTG (Fig. 5). After 4 h, cells were spun down. The vast majority of the protein was found in IB with a tiny amount in the soluble fraction. After washing the IB with buffer, the chimeric L1 was highly pure as seen on gels. Along with the 50kD full-length L1, a variable amount of 40 kD band was also observed in SDS-PAGE gels and on western blots. This was identified by LCMSMS to be outer membrane proteins (OMPs), which apparently sticks to IB. In the same band, variable amounts of a 40kD L1 degradation product were also found, as previously observed by others who expressed L1 in bacteria [35]. In addition to the dominant 40kD degradation product, we saw a smear in the western blot of lower molecular weight products. The size 40kD may correspond to the removal of the C-terminal 64-residue "invading arm" sequence. Since the invading arm binds capsomeres together to form the VLP, its loss could

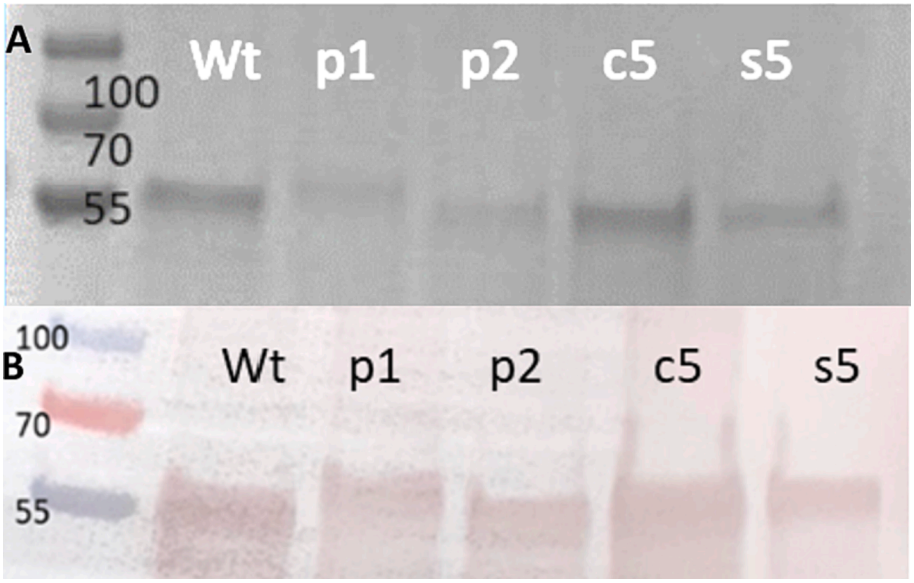

Fig. 5. Protein Expression and Isolation. A. SDS-PAGE of purified wild-type and chimeric CatSper-HPV L1 constructs from IB expression, labeled according to Table 1. B. Western blot of same proteins using anti-HPV L1 antibody CAMVIR1. WT, p1 and c5 constructs have slightly different masses.

be a source of the inconsistency in VLP formation.

Lysis by chemical methods (BPER, ThermoFisher Scientific, Waltham, MA, USA) led to a disappearance of the 50 kD L1 band from coomassie stained PAGE gels. BPER treatment of IB prepared by sonication led to the same disappearance. This disappearance could be reversed by the addition of urea to a final concentration of 4 M to the cell lysate prior to boiling in Laemli buffer for SDS-PAGE loading. Thus, the disappearance of the 50kD band was attributed to the resistance of the chemically "hardened" IB to SDS in boiling Laemli buffer.

3.6. In vitro folding and assembly

Each L1 variant was solubilized in 8 M urea, then refolded by pulsed-flash dilution under reducing conditions with a crowding agent, 0.1 M L-arginine. The refolded non-chimeric L1Δnls formed VLPs while dialyzing against high salt under oxidizing conditions, as shown by TEM (Fig. 6).

The bracketing CGP and GPC linkers around the inserted peptide are intended to provide conformational flexibility to the peptide, promoting a native-like structure, which is important for raising native-binding, neutralizing antibodies. The cysteines enable a disulfide bond that constrains the inserted loop into a cycle and helps mitigate any instability caused by the insertion . If formed, the disulfide would stabilize the final folded and assembled state.

If 6 M guanidine hydrochloride (GndHCl) was used instead of 8 M urea to solubilize the IB pellet, then more of the pellet was solubilized and less L1 was found in the pellet after the subsequent high speed spin. However, the GndHCl-denatured protein behaved differently during pulsed-flash dilution, precipitating more readily in the refolding buffer. This was not simply a result of a higher concentration of protein, as increasing the dilution factor 5-fold did not change the results. However, if GndHCl was used in small quantity (2 mL) to dissolve the IB, followed by 8 mL of urea, then nearly all of the IB could be dissolved, and the protein refolded from this mixed denaturant did not readily precipitate in the refolding buffer. We hypothesized that a portion of the IB is very tightly packed and resistant to urea solubilization. The different results upon flash dilution suggest that the unfolded state in 8 M urea is different from that of 6 M GndHCl, perhaps containing more residual native structure.

One hypothesis was that the GndHCl-denatured protein was trapped in a *cis*-peptide conformation, preventing folding. But when the same flash dilution was carried out in the presence of the prolyl-peptide isomerase cyclophilin A (CypA) [36], added to the refolding buffer at the appropriate pH and salt concentration, the results were no different. Therefore, the differences in the unfolded state are not due to peptide bond isomerization in the unfolded state. Although the protein dissolved using mixed denaturants could be successfully refolded to a soluble state, the protein did not assemble into VLPs. This method was tried repeatedly with nonchimeric L1Δnls and different chimeric constructs and never produced VLPs in TEM images. We concluded that solubilization in GndHCl must be avoided in order to assure VLP formation.

Both vigorous stirring and low temperature were required to avoid aggregation of the refolding protein. Vigorous stirring disperses the protein drops as they hit the refolding buffer, hopefully reducing the concentration to below the critical threshold for aggregation. Lower temperature has the expected Arrhenius behavior on aggregation rates, decreasing aggregation, in our observations. The results are consistent with the view of aggregation as competing with folding [37]. Aggregation tendency was observed to decrease with time since the start of refolding. The aggregate, when it forms, is therefore likely to be composed of partially folded states of the protein.

Successful formation of VLPs required dialyzing the refolded protein first in low salt (50 mM NaCl) then in high salt (300 mM or higher NaCl). It has been reported that capsomeres form at low salt but VLPs form only in high salt [38], a result of the highly negative charge on the capsomere substructures. During dialysis, if precipitation was observed, the protein was immediately spun at 15,000 g for 20 min to remove the aggregated material. If aggregates were removed in this way, then the remaining protein formed 60 nm VLPs.

3.7. Particle morphology and dispersity

TEM images for *p1* (Fig. 6D) and c5 (Fig. 6C) show morphologically normal VLPs, with visible capsomeres, indicating that the CatSper insertions do not interfere with L1 folding or assembly. The images also show aggregated protein in variable amounts. This aggregation is our protein, but in a misfolded or misassembled state.

The *s5* construct, containing the ps6 loop of CatSper1 inserted in the HI loop of L1 showed particles that have around the expected size and shape as expected from the DLS results. The DLS spectrum shown in Fig. 6F is representive of those constructs that show good VLPs in TEM (data not shown). Segmentation of the VLPs into capsomeres is faintly visible in these images. Also, numerous smaller particles are also present and it appears that the contrast agent, uranium acetate, does not enter the spheres. An amorphous aggregate would probably not have a consistently spherical shape by chance. Therefore, these are VLPs, but of a variable size.

Also found in the TEM studies was an abundance of non-VLP structures observed. Some appeared to be broken or partial VLPs. Some of the protein was in small regular particles, and in other cases it was found in large amorphous clumps. In one case (*p2*), the aggregate was soluble enough to inject mice, even though no VLPs were observed in the TEM. These structures indicate that our chimeric L1 samples contain forms of the protein that for some reason do not form complete VLPs. One possible explanation is that the C-terminal invading arms are frequently cleaved during expression and purification. The invading arms connect capsomeres. If an increased number of these connections are lost, it would make sense that VLPs would be increasingly rare. This represents an ongoing challenge.

3.8. Contraceptive efficacy

In the Round 1 mating experiment, 6–8 weeks old Balb/C female mice were immunized with vaccines *p1, p2, c5* and *s5*. All the vaccine candidates were found to be similarly immunogenic (Fig. 7), however only *p1* was contraceptive. Seven out of eight female Balb/C mice were protected from pregnancy (88 % efficacy) by antigen *p1*. Mouse 30, with a normal litter, had the lowest antibody concentration.

Data in Fig. 7 represents binding of antibodies raised against the chimeric L1 antigen, each containing one CatSper loop from Table 1, to KLH conjugates of the same loop. We found binding to the immobilized protein in all four cases. Since only the loop sequence is in common between the cL1 construct and the KLH conjugate, antibody binding must be to the inserted loop itself and not any other part of the cL1 VLPs. Controls showed no detectable binding to other loops, also on KLH.

The results for Round 1 revealed that all mice raised loop-specific antibodies, even though the loops were accompanied on the VLPs with some of the native HPV loops. No evidence of 'clonal dominance' [43] was observed, which would have produced some instances of antibodies against HPV loops only and no antibodies to the inserted loop. It is tempting to claim that the low loop-specific antibody concentration of mouse 30 (Fig. 7C) was responsible for this mouse being the only mouse in Round 1 not protected against pregnancy by *p1*.

Round 2 was intended to be the repeat of the Round 1 protocol, but using only the successful antigen, *p1*. But the experimented failed, as the negative control group had multiple animals without fetus (Table 1), and this taught us an important lesson. Consulting the manuals from Jackson Labs, we learned that the Balb/C strain has a comparatively lower fertility [53]. We believe that the failure of the negative control was a batch effect combined with low average fertility of Balb/C mice.

In Round 3, we replaced Balb/C with FVB/J mice which has a higher fertility rate. In this case there was no failure of the negative control; all

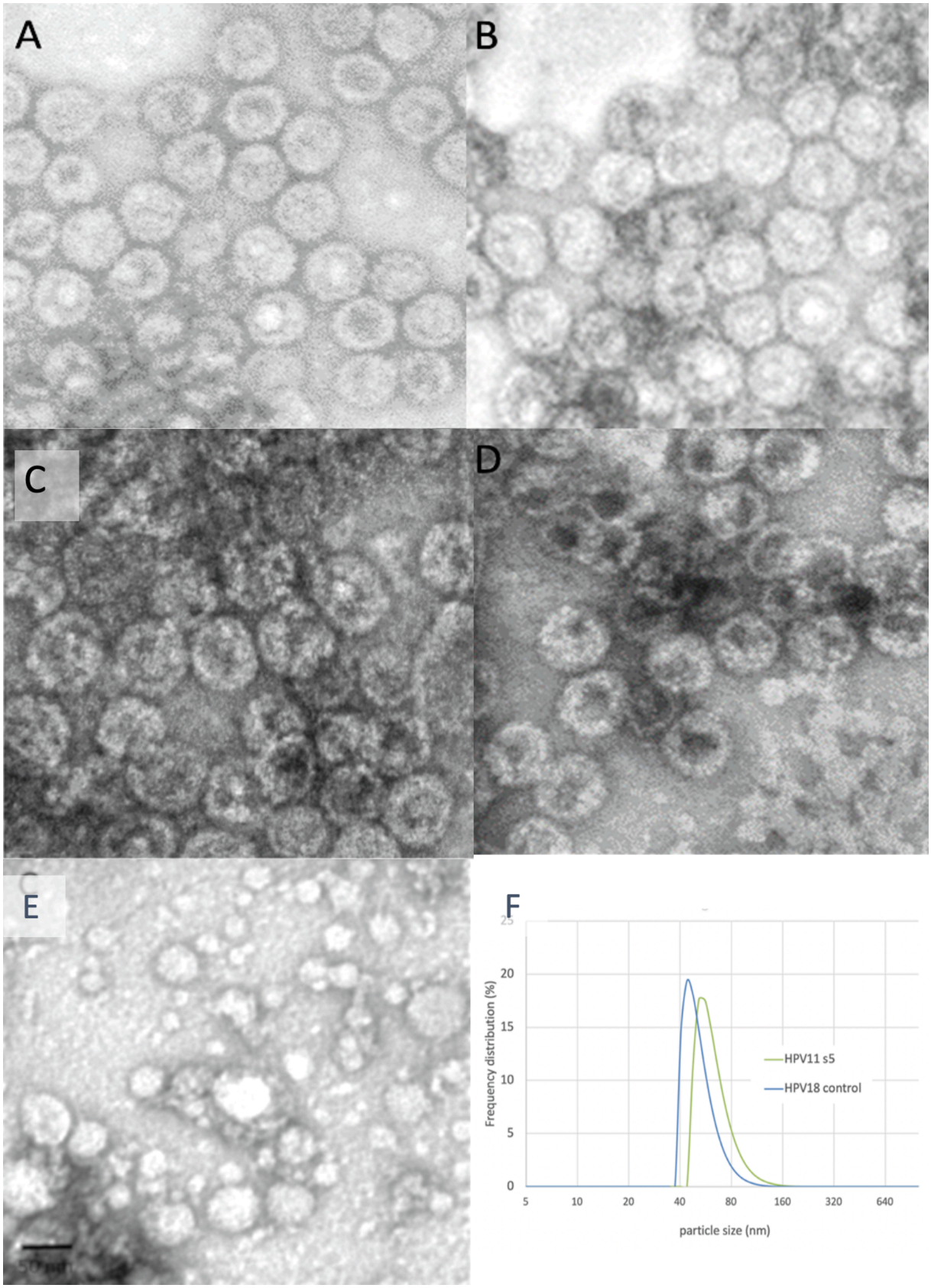

Fig. 6. 100000x images of uranyl acetate stained samples. Black bar is 50 nm. (A) Commercial HPV18 L1 VLPs. (B) L1Δnls with no insert. (C) *c5*, mCs*ε*_DGT inserted into the DE loop of L1Δnls. (D) *p1*, mCs1_s3s4 inserted into the BC loop of L1Δnls. (E) *s5*, mCs1_ps6 inserted into the HI loop of piL1.(F) DLS particle size frequency distribution for *s5* (green) and the control particles, HPV18 L1 (blue). (For interpretation of the references to colour in this figure legend, the reader is referred to the web version of this article.)

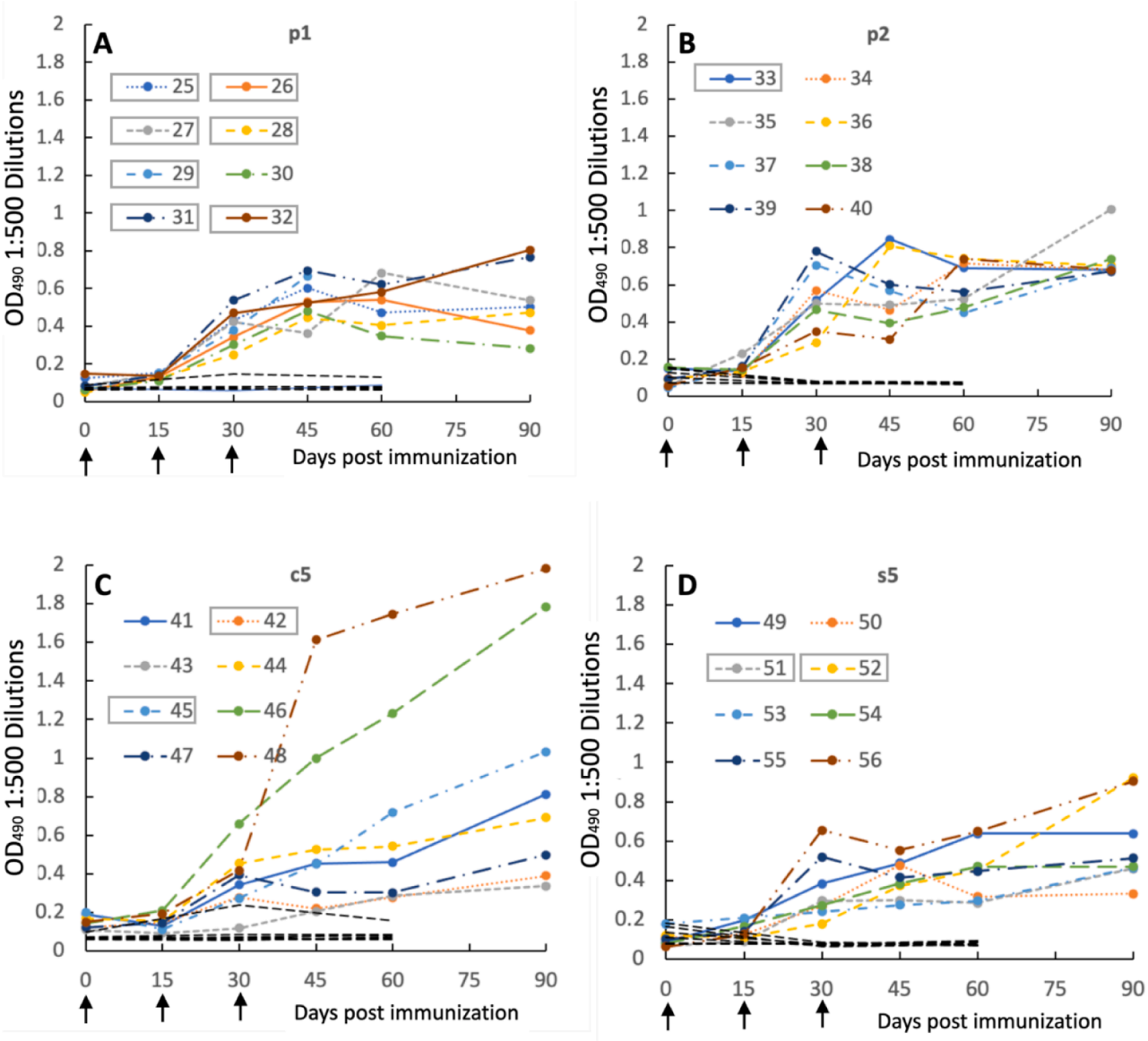

Fig. 7. Serum IgG determination at 1:500 dilution using ELISA coated with epitope-KLH antigen for round 1 vaccination groups of 8 Balb/C female mice each. Groups received 3 primary immunizations at day 0, 15 and 30 with different CatSper epitopes inserted into HPV L1 at hypervariable sites. (A) *p1* = mCs1_s3s4, (B) *p2* = mCs2_s1s2, (C) *c5* = mCsE_DGT and (D) *s5* = mCs1_ps6. Numbers in legends are mouse identities. Those boxed had zero embryos at Day 90. Unmarked black dashes are control measurements for each mouse at days 0, 30 and 60; wells were coated with KLH displaying an unrelated peptide. All data are averages of duplicates. Average absolute deviation between duplicates was 0.03. Significance of Day 30 or Day 60 OD's when compared to controls was $p < 0.01$ in each case.

8 had normal litters. In all, 4 out of 8 immunized mice were protected from pregnancy upon co-housing with males at a 2:1 ratio for three consecutive estrus cycles (50 % efficacy). Those females that did get pregnant had fetus numbers ranging from 5 to 12, which is not significantly different from normal litter size. We describe this as a black/white effect. Contraception is either complete or it is wholly absent. There were no small litters unless it was zero. Our initial guess to explain this phenomenon was that we were seeing clonal dominance in the B-cell maturation [46]where some individuals are focusing immunity on the CatSper loop and others are focusing immunity on HPV loops. However, loop-specific ELISA for Round 1 showed that all mice had loop-specific antibodies, arguing against clonal dominance.

3.9. Reversal

Although not tested in vivo, we have carried out ELISA-based proof of concept experiments for the reversal of the contraceptive effect. We modified a small protein, the C-terminal fragment of mouse serum albumin (mSAc) to act as a carrier for the *p1* loop. The recombinant protein was expressed in bacteria, purified using Ni-TED resin (Macherey-Nagel, GmbH &co, KG) and immobilized for ELISA. Specific binding to antibodies raised against *p1* chimeric HPV L1 was established. It has been reported that applying an adequate amount of a 12-residue peptide called YLP12 intravaginally was found to reverse the contraceptive effect raised by injecting a YLP12 -cholera toxin conjugate [51].

3.10. Antibody lifetime

For a contraceptive vaccine there is a strong interest in knowing the duration of the contraceptive immunity. We cannot say for sure how long our vaccine will last, but clinical trial data exists for unadulterated HPV vaccine (Gardasil) showing a lifetime in excess of 9 years, using various serotypes and mixtures of serotypes [50]. Our chimeric vaccine

is akin to a new serotype of HPV, having changes in the variable regions on the surface, and therefore we would expect our vaccines to have a long lifetime, like HPV. Other immunogenic carriers raise short or mediumterm immunity. For example, heat-labile enterotoxin subunit B (LTB) raises immunity to genetically fused loops but the immunity lasts only a few months. Tetanus toxin and diphtheria toxin raise immunity with an intermediate lifetime, 6 to 9 months, but are not approved for use in humans. Antibody lifetime is believed to be equivalent to the lifetime of the corresponding antibody-expressing B plasma cells, and the lifetime of these cells is believed to be a function of the antigen, where highly repetitive antigens such as viruses and VLPs lead to long-term immunity, while less repetitive, smaller, toxin molecules lead to short-term immunity [49].

3.11. Side effects

HPV vaccination is safe and effective, with few reported side effects. The most common side effect is soreness at the injection site. Severe allergic reactions following vaccination are rare, but can be life-threatening. Our vaccine is similar to HPV and is expected to have a similar rate of side effects. The sperm-derived loops that are genetically inserted will not induce autoimmunity in females or males since CatSper is expressed only in males and only in the testes, an immune-privileged organ. Only if the blood/testes barrier is breached by injury or surgery do we expect anti-CatSper antibodies to be manifested in the semen; if so the only autoimmunity in the male would be against CatSper in any case since the vaccine will contain no other human antigens. Sequence searches have found no similarity to other human proteins for any of the loops used here. The reveral agent is expected to have no side effects since it is non-immunogenic and because it will not be injected.

4. Conclusions

We have demonstrated proof of concept for chimeric HPV L1 as a carrier for a contraceptive peptide hapten. Chimeric L1 from bacterial inclusion bodies is highly pure and can fold and assemble into VLPs under the right conditions, but the process is sensitive to subtle changes and therefore not reliable. Refolding (pulse-flash dilution method) was sensitive to denaturant, reducing agent, temperature, protein concentration, salt concentration and to the specific sequence of the construct. TEM images showed well-formed VLPs for one construct (p1), poorly-formed VLPs in two cases (s5, c5) and soluble aggregate in one case (p2). All forms of the protein nonetheless raised antibodies.

VLPs carrying one of the CatSper extracellular loops showed a 50 % contraceptive effect in FVB/J mice, which is highly significant, albeit still uncompetitive in the contraception marketplace. Three other CatSper loops had no contraceptive effect. In the future we will try DNA priming [40] followed by the proteinic form of the vaccine to achieve higher antibody concentration, to attain full efficacy.

Declaration of Competing Interest

The authors declare the following financial interests/personal relationships which may be considered as potential competing interests: [Chris Bystroff reports financial support was provided by Grantham Foundation for the Protection of the Environment. Chris Bystroff reports a relationship with Grantham Foundation for the Protection of the Environment that includes: funding grants. Chris Bystroff has patent #US20220152166A1 issued to Rensselaer Polytechnic Institute.].

Data availability

No data was used for the research described in the article.

Acknowledgements

This research used resources of the Center for Functional Nanomaterials, which is a U.S. 531 DOE Office of Science Facility, at Brookhaven National Laboratory under Contract No. DE532 SC0012704, was funded by a gift from the Grantham Foundation for the Protection of the Environment to C.B. and J.-J.C.. and a grant from the National Institute of General Medical Sciences (R01GM099827) to C.B. Dr. Donna E. Crone provided consultation. Zeyuan Guo contributed to the laboratory work.

Appendix A. Supplementary data

Supplementary data to this article can be found online at https://doi.org/10.1016/j.vaccine.2023.09.044.

References

[1] Bearak J, Popinchalk A, Ganatra B, Moller AB, Tunçalp Ö, Beavin C, et al. Unintended pregnancy and abortion by income, region, and the legal status of abortion: estimates from a comprehensive model for 1990–2019. Lancet Glob Health 2020;8(9):e1152–61.
[2] Bradley SEK, Polis CB, Bankole A, Croft T. Global Contraceptive Failure Rates: Who Is Most at Risk? Stud Fam Plann 2019;50:3–24.
[3] Winner B, et al. Effectiveness of Long-Acting Reversible Contraception. The New England Journal of Medicine 2012;366:1998–2007.
[4] Mosher W, Jones J, Abma J. Nonuse of contraception among women at risk of unintended pregnancy in the United States. Contraception 2015;92:170–6.
[5] Sedgh G, Hussain R. Reasons for Contraceptive Nonuse among Women Having Unmet Need for Contraception in Developing Countries. Stud Fam Plann 2014;45:151–69.
[6] Dorman E, Bishai D. Demand for male contraception. Expert Rev Pharmacoecon Outcomes Res 2012;12:605–13.
[7] Naz, R. K. Antisperm Contraceptive Vaccine. in *Immune Infertility* 249–261 (Springer International Publishing, 2017). doi:10.1007/978-3-319-40788-3_17.
[8] Ohl DA, Naz RK. Infertility due to antisperm antibodies. Urology 1995;46:591–602.
[9] Nagaria T, Patra PK, Sahu JP. Evaluation of serum antisperm antibodies in infertility. J Obstet Gynecol India 2011;61:307–16.
[10] Baskin MJ. Temporary sterilization by the injection of human spermatozoa. A preliminary report. American Journal of Obstetrics and Gynecology 1932;24:892–7.
[11] Wang H, McGoldrick LL, Chung J-J. Sperm ion channels and transporters in male fertility and infertility. Nat Rev Urol 2021;18:46–66.
[12] Ren D, et al. A sperm ion channel required for sperm motility and male fertility. Nature 2001;413:603–9.
[13] Hwang JY, Wang H, Lu Y, Ikawa M, Chung J-J. C2cd6-encoded CatSperτ targets sperm calcium channel to Ca2+ signaling domains in the flagellar membrane. Cell Rep 2022;38:110226.
[14] Yang F, et al. C2CD6 regulates targeting and organization of the CatSper calcium channel complex in sperm flagella. Development 2022;149.
[15] Li H, Ding X, Guo C, Guan H, Xiong C. Immunization of male mice with B-cell epitopes in transmembrane domains of CatSper1 inhibits fertility. Fertil Steril 2012;97:445–52.
[16] Bystroff C. Intramembranal disulfide cross-linking elucidates the super-quaternary structure of mammalian CatSpers. Reprod Biol 2018;18:76–82.
[17] Lu Z, et al. Expression of Thioredoxin Random Peptide Libraries on the Escherichia coli Cell Surface as Functional Fusions to Flagellin: A System Designed for Exploring Protein-Protein Interactions. Nat Biotechnol 1995;13:366–72.
[18] Thönes N, Herreiner A, Schädlich L, Piuko K, Müller M. A direct comparison of human papillomavirus type 16 L1 particles reveals a lower immunogenicity of capsomeres than viruslike particles with respect to the induced antibody response. J Virol 2008;82:5472–85.
[19] Shank-Retzlaff ML, Zhao Q, Anderson C, Hamm M, High K, Nguyen M, et al. Evaluation of the thermal stability of Gardasil®. Hum Vaccin 2006;2(4):147–54.
[20] Lowy DR. HPV vaccination to prevent cervical cancer and other HPV-associated disease: from basic science to effective interventions. J Clin Invest 2016;126(1):5–11.
[21] Stemmer WPC, Crameri A, Ha KD, Brennan TM, Heyneker HL. Single-step assembly of a gene and entire plasmid from large numbers of oligodeoxyribonucleotides. Gene 1995;164:49–54.
[22] Guan J, et al. Cryoelectron Microscopy Maps of Human Papillomavirus 16 Reveal L2 Densities and Heparin Binding Site. Structure 2017;25:253–63.
[23] Okonechnikov K, Golosova O, Fursov M. Unipro UGENE: a unified bioinformatics toolkit. Bioinformatics 2012;28:1166–7.
[24] Edgar RC. MUSCLE: multiple sequence alignment with high accuracy and high throughput. Nucleic Acids Res 2004;32:1792–7.
[25] Ramakrishnan V, et al. Geofold: Topology-based protein unfolding pathways capture the effects of engineered disulfides on kinetic stability. ProteinsStruct Funct Bioinforma 2012;80:920–34.
[26] Li H, Ding X, Guan H, Xiong C. Inhibition of human sperm function and mouse fertilization in vitro by an antibody against cation channel of sperm 1: the

contraceptive potential of its transmembrane domains and pore region. Fertil Steril 2009;92:1141–6.
[27] Dartmann K, Schwarz E, Gissmann L, zur Hausen, H.. The nucleotide sequence and genome organization of human papilloma virus type 11. Virology 1986;151: 124–30.
[28] Li M, et al. Expression of the human papillomavirus type 11 L1 capsid protein in Escherichia coli: characterization of protein domains involved in DNA binding and capsid assembly. J Virol 1997;71:2988–95.
[29] Zhou J, et al. Identification of the nuclear localization signal of human papillomavirus type 16 L1 protein. Virology 1991;185:625–32.
[30] Hoover DM, Lubkowski J. DNAWorks: an automated method for designing oligonucleotides for PCR-based gene synthesis. Nucleic Acids Res 2002;30:43e–e.
[31] Laemmli UK. Cleavage of structural proteins during the assembly of the head of bacteriophage T4. Nature 1970;227(5259):680–5.
[32] Towbin H, Staehelin T, Gordon J. Electrophoretic transfer of proteins from polyacrylamide gels to nitrocellulose sheets: procedure and some applications. Proc Natl Acad Sci 1979;76(9):4350–4.
[33] Gundry RL, White MY, Murray CI, Kane LA, Fu Q, Stanley BA, et al. Preparation of proteins and peptides for mass spectrometry analysis in a bottomup proteomics workflow. Curr Protoc Mol Biol 2010;90(1):10–25.
[34] Deutsch EW, Mendoza L, Shteynberg D, Farrah T, Lam H, Tasman N, et al. A guided tour of the Trans-Proteomic Pipeline. Proteomics 2010;10(6):1150–9.
[35] Chen XS, Casini G, Harrison SC, Garcea RL. Papillomavirus capsid protein expression in Escherichia coli: purification and assembly of HPV11 and HPV16 L1. J Mol Biol 2001;307:173–82.
[36] Bhattacharyya R, Chakrabarti P. Stereospecific Interactions of Proline Residues in Protein Structures and Complexes. J Mol Biol 2003;331:925–40.
[37] Kiefhaber T, Rudolph R, Kohler H-H, Buchner J. Protein Aggregation in vitro and in vivo: A Quantitative Model of the Kinetic Competition between Folding and Aggregation. Nat Biotechnol 1991;9:825–9.
[38] McCarthy MP, White WI, Palmer-Hill F, Koenig S, Suzich JA. Quantitative disassembly and reassembly of human papillomavirus type 11 viruslike particles in vitro. J Virol 1998;72:32–41.
[39] Lin S, Ke M, Zhang Y, Yan Z, Wu J. Structure of a mammalian sperm cation channel complex. Nature 2021;595(7869):746–50.
[40] Nand KN, Gupta JC, Panda AK, Jain SK, Talwar GP. Priming with DNA enhances considerably the immunogenicity of hCG β-LTB vaccine. Am J Reprod Immunol 2015;74(4):302–8.
[41] Heesters BA, Myers RC, Carroll MC. Follicular dendritic cells: dynamic antigen libraries. Nat Rev Immunol 2014;14(7).
[42] Bystroff C, Baker D. Prediction of local structure in proteins using a library of sequence-structure motifs. J Mol Biol 1998;281(3):565–77.
[43] Schutze MP, Deriaud E, Przewlocki G, LeClerc C. Carrier-induced epitopic suppression is initiated through clonal dominance. J Immunol 1989;142(8): 2635–40.
[44] Varsani A, Williamson AL, De Villiers D, Becker I, Christensen ND, Rybicki EP. Chimeric human papillomavirus type 16 (HPV-16) L1 particles presenting the common neutralizing epitope for the L2 minor capsid protein of HPV-6 and HPV-16. J Virol 2003;77(15):8386–93.
[45] Mahmoodi M, Ghodsi M, Moghadam M, Sankian M. Pulsed Dilution Method for the Recovery of Aggregated Mouse TNF-α. Rep Biochem Mol Biol 2017 Apr;5(2): 103–7.
[46] Rayment I, Baker TS, Caspar DLD, Murakami WT. Polyoma virus capsid structure at 22.5 Å resolution. Nature 1982;295(5845):110–5.
[47] Carrillo-Tripp M, Shepherd CM, Borelli IA, Venkataraman S, Lander G, Natarajan P, et al. VIPERdb2: an enhanced and web API enabled relational database for structural virology. Nucleic Acids Res 2009;37(suppl_1):D436–42.
[48] Albus U. Guide for the care and use of laboratory animals. (8th edn). 2012.
[49] Slifka MK, Amanna IJ. Role of multivalency and antigenic threshold in generating protective antibody responses. Front Immunol 2019;10:956.
[50] Bonanni P, Boccalini S, Bechini A. Efficacy, duration of immunity and cross protection after HPV vaccination: a review of the evidence. Vaccine 2009;27: A46–53.
[51] Naz RK, Chauhan SC. Human sperm-specific peptide vaccine that causes longterm reversible contraception. Biol Reprod 2002;67(2):674–80.
[52] De Winter JC. Using the Student's t-test with extremely small sample sizes. Pract Assess Res Eval 2019;18(1):10.
[53] Taketo M, Schroeder AC, Mobraaten LE, Gunning KB, Hanten G, Fox RR, et al. FVB/N: an inbred mouse strain preferable for transgenic analyses. Proc. Natl. Acad. Sci. 1991;88(6):2065–9.